ELSEVIER

Available at WWW.MATHEMATICSWEB.ORG POWERED BY SCIENCE DIRECT®

Journal of Computational and Applied Mathematics 157 (2003) 309–327

JOURNAL OF COMPUTATIONAL AND APPLIED MATHEMATICS

www.elsevier.com/locate/cam

# A new approximate matrix factorization for implicit time integration in air pollution modeling☆

M.A. Botchev[a,*], J.G. Verwer[b]

[a] *Department of Applied Mathematics, University of Twente, P.O. Box 217, 7500 AE Enschede, The Netherlands*
[b] *CWI, P.O. Box 94079, 1090 GB Amsterdam, The Netherlands*

Received 3 April 2002; received in revised form 18 December 2002

**Abstract**

Implicit time stepping typically requires solution of one or several linear systems with a matrix $\boldsymbol{I}-\tau\boldsymbol{J}$ per time step where $\boldsymbol{J}$ is the Jacobian matrix. If solution of these systems is expensive, replacing $\boldsymbol{I}-\tau\boldsymbol{J}$ with its approximate matrix factorization (AMF) $(\boldsymbol{I}-\tau\boldsymbol{R})(\boldsymbol{I}-\tau\boldsymbol{V})$, $\boldsymbol{R}+\boldsymbol{V}=\boldsymbol{J}$, often leads to a good compromise between stability and accuracy of the time integration on the one hand and its efficiency on the other hand. For example, in air pollution modeling, AMF has been successfully used in the framework of Rosenbrock schemes. The standard AMF gives an approximation to $\boldsymbol{I}-\tau\boldsymbol{J}$ with the error $\tau^2\boldsymbol{R}\boldsymbol{V}$, which can be significant in norm. In this paper we propose a new AMF. In assumption that $-\boldsymbol{V}$ is an $M$-matrix, the error of the new AMF can be shown to have an upper bound $\tau\|\boldsymbol{R}\|$, while still being asymptotically $\mathcal{O}(\tau^2)$. This new AMF, called AMF+, is equal in costs to standard AMF and, as both analysis and numerical experiments reveal, provides a better accuracy. We also report on our experience with another, cheaper AMF and with AMF-preconditioned GMRES.


*MSC:* 65M06; 65M20; secondary: 62Y20

*Keywords:* Operator splitting; Approximate matrix factorization; Large sparse linear systems; Stiff ODEs; Method of lines; Rosenbrock methods; Air pollution modeling; GMRES; Krylov solvers

## 1. Introduction

Typically, in air pollution modeling systems of millions of stiff ODEs, describing advection, vertical mixing by vertical diffusion and cloud transport and reactions of the trace gases, have to be integrated in time on intervals ranging from months to years [35,37].

☆ This work has been sponsored by the Netherlands Organization for Scientific Research (NWO).
* Corresponding author. Tel.: +31-534893396; fax: +31-5348u94833.
*E-mail addresses:* m.a.botchev@math.utwente.nl (M.A. Botchev), jan.verwer@cwi.nl (J.G. Verwer).

0377-0427/03/$ - see front matter 
doi:10.1016/S0377-0427(03)00414-X

The huge scale of air pollution problems suggests the use of special time integration, e.g. the widely used operator splitting, where the physical processes are handled separately. Normally, vertical mixing and reactions are stiff processes and thus require implicit time stepping. On the other hand, the step sizes used for these processes usually lead to CFL numbers below 1 for advection. Therefore, when operator splitting is used, it is natural to apply an explicit scheme for advection and implicit schemes for reactions and vertical mixing. Operator splitting is, however, not always a fortunate choice in the stiff case because the splitting error may spoil the solution. This is especially pronounced for the fast varying trace gases (the so-called radicals) [2–4,30].

The most straightforward way to avoid splitting while still treating advection explicitly is to apply an implicit scheme, say a Rosenbrock scheme [6,12], with a Jacobian containing entries of only reactions and vertical mixing terms. Another alternative is to use the so-called source splitting [15–17], where the advection step is performed first and added as the source during the implicit vertical mixing-reaction substep. In both cases Rosenbrock schemes are attractive because they have nice stability properties, often readily allow inexact Jacobians and require a fixed number of linear solves per time step.

The standard off-the-shelf ODE solvers based on implicit multistep or Runge–Kutta formulas and Newton iteration are typically not efficient for air pollution problems [28,35,37]. The accuracy requirements for these problems are very modest and simple second- or third-order Rosenbrock schemes with a fixed step size often turn out to be the best choice [27].

The semi-discrete ODE system representing the coupled vertical mixing-reaction process can be written as

$$\dot{\boldsymbol{y}} = \boldsymbol{f}(\boldsymbol{y}), \quad \boldsymbol{f}(\boldsymbol{y}) = \boldsymbol{V}\boldsymbol{y} + \boldsymbol{r}(\boldsymbol{y}), \quad \boldsymbol{y} \in \mathbb{R}^N, \quad N = n_z n_t, \tag{1}$$

where $\boldsymbol{V}$ is the vertical mixing matrix, $\boldsymbol{r}(\boldsymbol{y})$ is the reaction term, $n_z$ is the number of vertical layers and $n_t$ is the number of trace gases. Typically, $20 \leqslant n_z \leqslant 50$ and $20 \leqslant n_t \leqslant 100$. The linear systems arising in linearly implicit schemes applied to (1) have the form

$$(\boldsymbol{I} - \tau\boldsymbol{J})\boldsymbol{x} = \boldsymbol{b}, \quad \boldsymbol{x}, \boldsymbol{b} \in \mathbb{R}^N, \tag{2}$$

where $\boldsymbol{J}$ is Jacobian of the reactions and vertical mixing, $\tau = \gamma\,\Delta t$, $\gamma$ is a parameter of the Rosenbrock scheme, $\Delta t$ is the step size. In the following we write $\boldsymbol{J} = \boldsymbol{V} + \boldsymbol{R}$ where $\boldsymbol{R}$ is a Jacobian matrix $\partial \boldsymbol{r}(\boldsymbol{y})/\partial \boldsymbol{y}$ evaluated at a certain point.

A serious computational bottleneck is caused by the fact that $\boldsymbol{J}$ usually has a structure that prevents the efficient direct solution of (2). The matrix $\boldsymbol{I} - \tau\boldsymbol{J}$ is rather large, of size $N$ up to $10^4$, and sparse (see Fig. 1) but the sparsity would be largely lost during the LU factorization and thus the costs of the factorization as well as of the backsolves would be dramatically increased. Increase of the costs is often simply not feasible, since in air pollution models one has many independent linear systems (2). Normally there is one system (2) per horizontal grid location, i.e., there are altogether $n_x \times n_y$ systems, where $n_x$, $n_y$ are horizontal grid size dimensions.

A natural way to avoid the expensive LU solve for linear systems (2) is to settle for an approximate solution. As proposed in [36], for air pollution models this can be done with the help of approximate matrix factorization (AMF)

$$\boldsymbol{I} - \tau\boldsymbol{J} \approx (\boldsymbol{I} - \tau\boldsymbol{R})(\boldsymbol{I} - \tau\boldsymbol{V}), \tag{3}$$

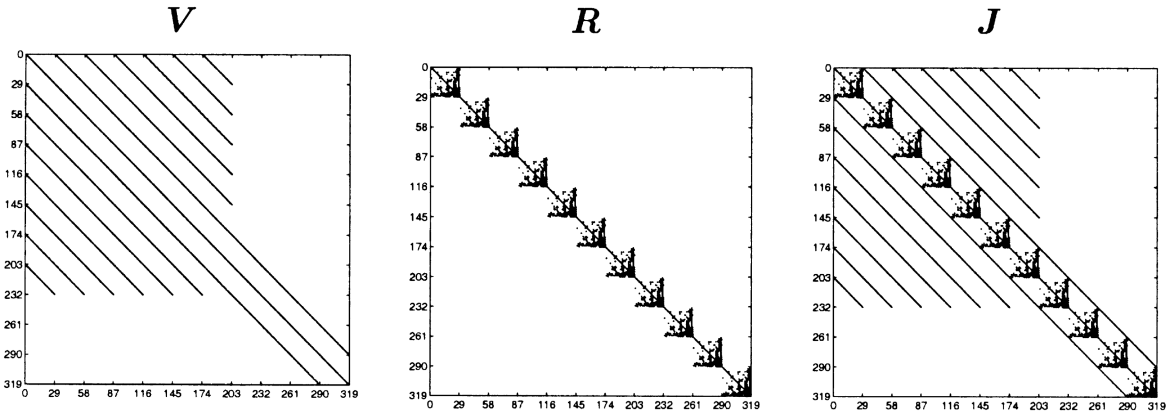


Fig. 1. Sparsity structure of the vertical mixing matrix $\boldsymbol{V}$, the reaction Jacobian $\boldsymbol{R}$ and the coupled vertical mixing-reaction system Jacobian $\boldsymbol{J} = \boldsymbol{V} + \boldsymbol{R}$ for $n_t = 29$ and $n_z = 11$. The $n_z$ diagonal blocks of $\boldsymbol{R}$ are of size $n_t \times n_t$ and correspond to the chemistry Jacobians per grid point.

by computing $\boldsymbol{x}$ as

$$\boldsymbol{x} := (\boldsymbol{I} - \tau \boldsymbol{V})^{-1}(\boldsymbol{I} - \tau \boldsymbol{R})^{-1}\boldsymbol{b}. \tag{4}$$

AMF was introduced in [1,7]. However, the idea of AMF can already be seen in the alternating direction implicit (ADI) method of Peaceman and Rachford [21]. Apart from [36], recent papers on AMF in implicit time integration include [10,14,18,19,33].

The nice property of AMF is that, when AMF is used within a Rosenbrock scheme applied to the coupled vertical mixing-reactions system, the total computational expenses are just the same as when the Rosenbrock scheme is applied first to vertical mixing and then to reactions within the operator splitting. This was exploited in [36], where a second order $L$-stable Rosenbrock scheme ROS2 (see [6, Chapter 9]) was successfully applied in combination with AMF to different test problems typical for air pollution modeling. The ROS2 scheme can be written as

$$\begin{aligned}
&\boldsymbol{y}^{n+1} = \boldsymbol{y}^n + \tfrac{3}{2}\boldsymbol{k}_1 + \tfrac{1}{2}\boldsymbol{k}_2,\\
&(\boldsymbol{I} - \gamma\,\Delta t \boldsymbol{A})\boldsymbol{k}_1 = \Delta t \boldsymbol{f}(\boldsymbol{y}^n),\\
&(\boldsymbol{I} - \gamma\,\Delta t \boldsymbol{A})\boldsymbol{k}_2 = \Delta t \boldsymbol{f}(\boldsymbol{y}^n + \boldsymbol{k}_1) - 2\boldsymbol{k}_1.
\end{aligned} \tag{5}$$

This two-stage method is second-order consistent for any matrix $\boldsymbol{A}$. The matrix $\boldsymbol{A}$ is supposed to be an approximation to the Jacobian matrix $\boldsymbol{J} = \boldsymbol{f}'(\boldsymbol{y}^n)$. If the AMF approximation is used, one chooses $\boldsymbol{A}$ such that

$$\boldsymbol{I} - \tau \boldsymbol{A} = (\boldsymbol{I} - \tau \boldsymbol{R})(\boldsymbol{I} - \tau \boldsymbol{V}), \quad \tau = \gamma\,\Delta t.$$

When using the exact Jacobian, the method has a stability function which is $A$-stable for $\gamma \geqslant \frac{1}{4}$ and $L$-stable for $\gamma = 1 \pm \frac{1}{\sqrt{2}}$. The two-stage scheme (5) can be made third-order accurate and $A$-stable by adapting the coefficients [18,19]. Third-order accuracy does however require that $\boldsymbol{A} = \boldsymbol{J} + \mathcal{O}(\tau)$

which is not necessary for second order. This so-called ROS3 scheme has been successfully used in combination with AMF [18,19].

An important point is that incorporation of AMF largely preserves stability. ROS2-AMF retains $A$-stability, only $L$-stability is lost [36]. In [2,4], this ROS2-AMF scheme was tested against the standard operator Strang splitting in the framework of two real-life air pollution models, the regional LOTOS model [20] and the global TM3 model [31]. The test problems in [2,4] were different, e.g., there was no advection in [2] while on the other hand there was no cloud transport in [4]. However, in both situations, within the same amount of computational work, ROS2-AMF gave a better, more accurate solution than operator splitting and source splitting. A possible alternative to AMF for the approximate solution of the linear system (2) might be a modern Krylov iterative solver. This is further discussed in Section 4.2.

In this paper we propose a new AMF. This new AMF, refered to as AMF+, is aimed at improving AMF qualitatively. The standard AMF gives an approximation to $\boldsymbol{I}-\tau\boldsymbol{J}$ with the error $\tau^2\boldsymbol{R}\boldsymbol{V}$, which can be significant in norm in the stiff case. This means that the accuracy of an AMF-based scheme can be inferior due to the approximate factorization, especially for the "stiff" trace gases. AMF+ is constructed to relieve this problem. Assuming that $-\boldsymbol{V}$ is a columnwise diagonally dominant $M$-matrix [1] (this assumption is briefly discussed in the next section), we show that the error of AMF+, while still being asymptotically $\mathcal{O}(\tau^2)$, has an upper bound $\tau\|\boldsymbol{R}\|_1$. AMF+ requires the same computational costs as standard AMF and, as numerical experiments reveal, provides a more accurate solution. The analysis suggests that the more diagonally dominant the matrix $-\boldsymbol{V}$ is, the larger the profit provided by AMF+.

The structure of the paper is as follows. In Section 2 we give more details relevant to the topic. Section 3 describes AMF+. In Section 4, two other possibilities to solve systems (2) are discussed, namely (i) a cheaper variant of AMF and (ii) an preconditioned iterative solver. The results of numerical tests are discussed in Section 5 and, finally, the conclusions are drawn in Section 6.

## 2. Vertical mixing matrix, reaction Jacobian and AMF

For typically used step sizes ($\approx 30$ min) one has

$$\Delta t\|\boldsymbol{V}\|_2 \sim \mathcal{O}(10), \quad \Delta t\|\boldsymbol{R}\|_2 \sim \mathcal{O}(10^6), \tag{6}$$

whereas smallest in modulus eigenvalues of both of the matrices multiplied with the step size are of order $\mathcal{O}(10^{-5})$. This illustrates the stiffness of the problem and thus the need of (linearly) implicit time integration for the vertical mixing-reaction part.

The sparsity structure of $\boldsymbol{V}$ shown in Fig. 1 corresponds to the following ordering of unknowns in the vector $\boldsymbol{x}$ (cf. (2)):

$$\boldsymbol{x} = \{x_{km}\}, \quad k = 1,\ldots,n_z, \quad m = 1,\ldots,n_t,$$

$$\boldsymbol{x} = (x_{11}, x_{12}, \ldots, x_{1n_t}, \ldots, x_{n_z1}, x_{n_z2}, \ldots, x_{n_zn_t}).$$

[1] Matrix $A$ is called an $M$-matrix if $A = sI - B$ where matrix $B$ is elementwise nonnegative and $s > \rho(B)$, $\rho(B)$ being the spectral radius of $B$. $A$ is a singular $M$-matrix if $s = \rho(B)$.

With another ordering, namely with

$$\boldsymbol{x} = (x_{11}, x_{21}, \ldots, x_{n_z 1}, \ldots, x_{1 n_t}, x_{2 n_t}, \ldots, x_{n_z n_t}), \tag{7}$$

the matrix $\boldsymbol{V}$ transforms to a block-diagonal matrix with $n_z \times n_z$ dense diagonal blocks $V_m$, $m = 1, \ldots, n_t$. Each block $V_m$ describes the vertical mixing process of the trace gas number $m$. Often

$$V_m = \text{const}(m), \tag{8}$$

i.e., all trace gases are mixed in the same way. In the TM3 and TM5 global models [31,32], where the vertical mixing operator also includes the so-called scavenging (i.e. washing out) process, matrices $V_m$ do depend on $m$. With only vertical diffusion present in the vertical mixing process, all matrices $V_m$ would be tridiagonal if it is assumed that the three-point discretization is used. Unlike vertical diffusion, the cloud transport couples vertical layers in the model in a nonlocal manner thus causing the matrices $V_m$ to be dense.

Analysis of the new AMF+ is made in assumption that $-\boldsymbol{V}$ is an (possibly singular) $M$-matrix. This assumption is in general not satisfied in real air pollution models but does hold (see [2,13]) for the operational air pollution models TM3/TM5 [31,32] which motivated our study. If $-\boldsymbol{V}$ is not an $M$-matrix our analysis, in particular estimate (11), does not remain true. However, we do not see any reason why in this case the new AMF+ would be inferior to the standard AMF. For both AMF and AMF+, one may expect that failure of $-\boldsymbol{V}$ to be an $M$-matrix will make pivoting in LU factorization of $\boldsymbol{I} - \tau \boldsymbol{V}$ necessary to avoid possible numerical stability problems. The LU factorization of $\boldsymbol{I} - \tau \boldsymbol{V}$ needed to compute $\boldsymbol{x}$ in (4) is done blockwise for each of the blocks $I - \tau V_m$. This costs $\mathcal{O}(n_t n_z^3)$ operations, or $\mathcal{O}(n_z^3)$ operations when all the blocks $V_m$ are identical.

The reaction Jacobian $\boldsymbol{R}$ is a block-diagonal matrix with sparse diagonal blocks $R_k$, $k = 1, \ldots, n_z$, which are reaction Jacobians in a cell $k$ (cf. Fig. 1). The sparsity of the blocks can be efficiently exploited in the course of the LU factorization of $\boldsymbol{I} - \tau \boldsymbol{R}$. Using a special preprocessor tool kinetic preprocessor (KPP, [26]), an optimal ordering of the trace gases can be found for which the $\boldsymbol{L}$ and $\boldsymbol{U}$ factors are as sparse as possible. In practice this means that the matrix $\boldsymbol{L} + \boldsymbol{U}$ usually has only few percent more fill-in than $\boldsymbol{I} - \tau \boldsymbol{R}$. This optimal ordering is kept fixed during all time steps and no pivoting is used in the LU factorization of $\boldsymbol{I} - \tau \boldsymbol{R}$. This has become a common practice when using KPP and normally is not observed to cause serious stability problems (for further discussion see [26]).

Preserving sparsity of the reaction Jacobian is crucial and, in general, leads to certain limitations in the choice of an efficient approximate solver for (2). For example, for the case where cloud transport is absent and thus $\boldsymbol{V}$ is tridiagonal, one could choose for the full LU factorization of $\boldsymbol{I} - \tau \boldsymbol{J}$ to be performed blockwise. This would however distort sparsity within the blocks, so that the computational work would increase unacceptably.

## 3. AMF+: improving AMF

### 3.1. Definition of AMF+

We call AMF+ the following approximation to $\boldsymbol{I} - \tau \boldsymbol{J}$:

$$\boldsymbol{I} - \tau \boldsymbol{J} \approx (\boldsymbol{L}_V - \tau \boldsymbol{R}) \boldsymbol{U}_V, \quad \boldsymbol{L}_V \boldsymbol{U}_V = \boldsymbol{I} - \tau \boldsymbol{V}, \tag{9}$$

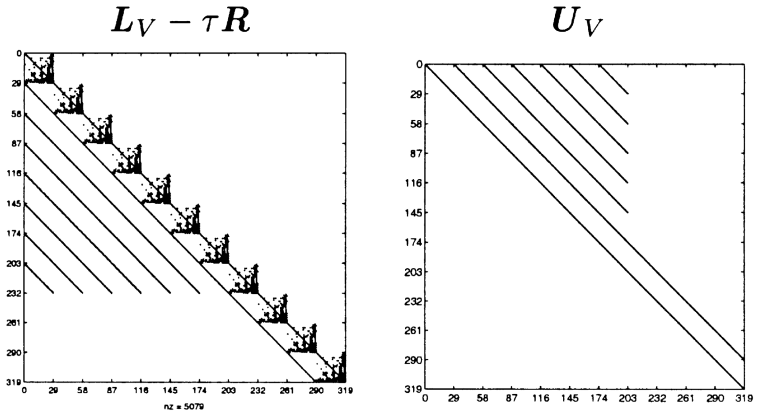


Fig. 2. Sparsity structure of the AMF+ matrix factors.

where $L_V$ and $U_V$ are the LU factors of $I-\tau V$ and $\tau=\gamma\,\Delta t$ ($\gamma$ is the Rosenbrock scheme parameter). The sparsity portraits of the AMF+ factors $L_V-\tau R$ and $U_V$ are shown in Fig. 2. Both factors can be easily inverted since $U_V$ is triangular and $L_V-\tau R$ is block triangular. To invert the diagonal blocks of $L_V-\tau R$, sparse LU factorization is used, in the same way as in the standard AMF for inversion of blocks in $I-\tau R$.

As discussed above, for our analysis we assume that $-V$ is a columnwise weakly diagonally dominant $M$-matrix, or a singular $M$-matrix with zero column sums. (These properties are not guaranteed in general but do hold [2] in the TM3/TM5 models. From the relation

$$(L_V-\tau R)U_V = I-\tau V-\tau R U_V = I-\tau J+\tau R(I-U_V), \tag{10}$$

we see that the error term $\tau R(I-U_V)$ does not seem to be of second order in $\tau$. Nevertheless it will be of second order if we use the freedom to choose the diagonal elements in one of the LU factors and take

$$\mathrm{Diag}(U_V)=I.$$

The matrix $I-U_V$ is then strictly upper triangular with entries $\mathcal{O}(\tau)$. This can be proven by mathematical induction with respect to the size of the matrix.

While for small $\tau$ the AMF+ error term behaves as $\mathcal{O}(\tau^2)$, for large $\tau$ it grows at most linearly in $\tau$. This can be seen from the fact that $U_V$ inherits the columnwise diagonal dominance from $I-\tau V$ and therefore

$$\|I-U_V\|_1<1,$$

so that the norm of the AMF+ error can be estimated as

$$\tau\|R(I-U_V)\|_1 \leqslant \tau\|R\|_1\|I-U_V\|_1 < \tau\|R\|_1. \tag{11}$$

A similar estimate, but in the maximum-row norm $\|*\|_\infty$ can be obtained if $-V$ is a rowwise weakly diagonally dominant $M$-matrix or a singular $M$-matrix with zero row sums.

In fact, $\|I-U_V\|_1$ can be rather small in practice and here lies the main attractiveness of AMF+. As an illustration, consider the case where the diagonal block $V$ of the matrix $V$, representing

vertical mixing of one trace gas (cf. (7) and (8)), is a tridiagonal matrix:

$$I-\tau V=\begin{bmatrix} a_1 & -b_1 & & 0 \\ -b_1 & a_2 & \ddots & \\ & \ddots & \ddots & -b_{n_z-1} \\ 0 & & -b_{n_z-1} & a_{n_z} \end{bmatrix}, \quad a_k>0, \quad b_k\geqslant 0, \quad k=1,\dots,n_z. \tag{12}$$

Since $V$ is either (weakly) diagonally dominant or has zero column sums, we have

$$a_k-b_k-b_{k-1}=\delta_k\geqslant 1, \quad k=1,\dots,n_z, \tag{13}$$

where it is assumed that $b_0=b_{n_z}=0$. It is easy to check that

$$I-\tau V=L_V U_V, \quad U_V=\begin{bmatrix} 1 & -u_1 & & 0 \\ 0 & 1 & \ddots & \\ & \ddots & \ddots & -u_{n_z-1} \\ 0 & & 0 & 1 \end{bmatrix},$$

$$u_1=\frac{b_1}{a_1}, \quad u_k=\frac{b_k}{a_k-b_{k-1}u_{k-1}}, \quad k=2,\dots,n_z$$

and, taking into account (13)

$$0\leqslant u_k=\frac{b_k}{a_k-b_{k-1}u_{k-1}}\leqslant\frac{b_k}{a_k-b_{k-1}}=\frac{b_k}{b_k+\delta_k}. \tag{14}$$

We see that $u_k$ can be small if the $\delta_k$ are sufficiently large, in other words, if $I-\tau V$ is "sufficiently" diagonally dominant. Estimates on entries of $U_V$ similar to (14) can also be obtained for more general situations where $I-\tau V$ is not tridiagonal. Note that similar estimates for the error term of the standard AMF would not be possible (cf. (21)).

### 3.2. A simple stability analysis

Since in AMF+ we deal with triangular matrices, to analyze the stability of a Rosenbrock method applied with AMF+ we cannot consider the usual scalar test equation $\dot{y}=\lambda y$. Analyzing stability of higher order Rosenbrock methods for the more general test case, a *system* of linear ODEs $\dot{y}=Jy$, does not seem an easy task when an approximate Jacobian $A(\approx J)$ is involved, which does not commute with $J$. We are able to perform stability analysis only for the first order Rosenbrock scheme combined with AMF+. Let us consider the following two linear test systems of $n_z$ ODEs:

$$\dot{y}=Jy, \quad J=V+D, \quad D=\mathrm{Diag}(\lambda_1,\dots,\lambda_{n_z}), \tag{15}$$

$$\dot{y}=Jy, \quad J=V+\lambda I, \tag{16}$$

where $\lambda < 0$, $\lambda_k < 0$ $(k = 1, \ldots, n_z)$, and $V$ is a symmetric negative semidefinite matrix:

$$V = V^{\mathrm{T}} \leqslant 0.$$

Henceforth, matrix inequalities of the form $A < B$ $(A > B)$ mean that matrix $A - B$ is negative definite (respectively, positive definite) in the real vector space with standard inner product $(x, y) = x^{\mathrm{T}} y$. Note that $A - B$ is not required to be symmetric.

Both test problems (15) and (16) are simplified versions of the vertical mixing-reaction problems as they occur in air pollution models. There are two assumptions under which the reduction to (15) is possible. The first one is that the vertical mixing process is described by the same matrix $V_m = V$ for all trace gases $m$ (this can be the case even in full-scale operational models). The second assumption is that the reaction process is linear and the reaction matrix $\boldsymbol{R}$ (cf. Fig. 1) has diagonal blocks with *the same* full set of eigenvectors. Diagonalization of $\boldsymbol{R}$ then would lead us to $n_t$ uncoupled test problems (15), one for each trace gas. Under a stronger assumption, that blocks of $\boldsymbol{R}$ are identical, these $n_t$ systems would have the form (16). Note that only in the latter case $\boldsymbol{RV} = \boldsymbol{VR}$.

The first-order Rosenbrock scheme (which we will denote by ROS1) applied to a linear system of ODEs $\dot{y} = Jy$ can be written as

$$y^{n+1} = Sy^n, \quad S = B^{-1}(B + \tau J), \quad B \approx I - \tau J, \tag{17}$$

where $\tau = \Delta t$ is the step size and the approximation $B$ is computed by AMF. Assume that $J$ is symmetric and negative definite. We introduce the so-called "energy" vector and matrix norms as

$$\|y\|_J = \sqrt{(-Jy, y)},$$

$$\|S\|_J^2 = \inf\{M \mid (-JSy, Sy) \leqslant M(-Jy, y)\}.$$

We use the following result on stability of ROS1 due to Samarskii [11,24,25]:

Stability criterion. *Assume that* $J = J^{\mathrm{T}} < 0$ *and* $B > 0$. *Then the scheme* (17) *is stable, i.e.*

$$\|S\|_J \leqslant 1$$

*if and only if*

$$B + \frac{\tau}{2} J \geqslant 0. \tag{18}$$

(*Note that B is not required to be symmetric.*)

We analyze stability of ROS1-AMF+ using the test problems (15), (16) and stability condition (18). With

$$B = (L_V - \tau R)U_V, \quad L_V U_V = I - \tau V,$$

we will check whether the matrix $B + (\tau/2)J$ is positive definite:

$$B + \frac{\tau}{2} J = L_V U_V - \tau R U_V + \frac{\tau}{2} V + \frac{\tau}{2} R = I - \frac{\tau}{2} V + \frac{\tau}{2} R(I - 2U_V).$$

Since $V = V^{\mathrm{T}} < 0$, the matrix $I - (\tau/2)V$ is positive definite. Consider the last term, $(\tau/2)R(I - 2U_V)$. This term can be large because $R$ is a "stiff" reaction matrix. Since $R$ is negative definite, one might hope that $(\tau/2)R(I - 2U_V)$ is positive definite if $I - 2U_V$ is negative semidefinite. However, it is not negative semidefinite for arbitrary matrices $V$ from the class we are considering (namely, matrices

$V$ such that $-V$ is a (singular) Stieltjes matrix [2] with columnwise weak diagonal dominance or zero column sums):

**Lemma 1.**

$$\{((I-2U_V)x,x)\,|\,(x,x)=1\}\subset(-3,1). \tag{19}$$

**Proof.**

$$((I-2U_V)x,x)=(x,x)-2\tfrac{1}{2}((U_V+U_V^{\mathrm{T}})x,x)=(x,x)-(\hat{U}x,x),$$

where the matrix $\hat{U}=U_V+U_V^{\mathrm{T}}$ is a symmetric irreducibly diagonally dominant matrix with 2 as main diagonal entries: $\hat{D}=\mathrm{Diag}(\hat{U})=2I$. It is easy to check that

$$(x,x)-(\hat{U}x,x)=-(x,x)+2((I-\hat{D}^{-1}\hat{U})x,x).$$

Since $I-\hat{D}^{-1}\hat{U}$ is the Jacobi iteration matrix of the diagonally dominant matrix $\hat{U}$, its spectral radius is less than one and

$$-2(x,x)\leqslant 2((I-\hat{D}^{-1}\hat{U})x,x)\leqslant 2(x,x),$$

because $I-\hat{D}^{-1}\hat{U}$ is symmetric. □

We can guarantee that $I-2U_V$ is negative definite for the following class of tridiagonal matrices $I-\tau V$:

**Lemma 2.** *Let $I-\tau V$ be a tridiagonal diagonally dominant matrix given by* (12), (13) *and*

$$\delta_k\geqslant b_k,\quad k=1,\dots,n_z-1. \tag{20}$$

*Then the matrix $I-2U_V$ is negative definite.*

**Proof.** It is easy to check that (14) and (20) guarantee that

$$u_k\leqslant\tfrac{1}{2},\quad k=1,\dots,n_z.$$

Define matrix $\hat{U}$ as in the proof of Lemma 1. Then we have

$$((2U_V-I)x,x)=((\hat{U}-I)x,x)>0,$$

because the diagonal entries of $\hat{U}$ are equal to 2 and its off-diagonal entries do not exceed $\frac{1}{2}$, so that the matrix $\hat{U}-I$ is irreducibly diagonally dominant. □

**Lemma 3.** *The assumptions of Lemma 2 on $I-\tau V$ are fulfilled for any $\tau>0$ if $V$ stems from the standard second-order finite difference approximation*

$$[(Ku_z)_z]_k\approx\frac{K_{k+1/2}(u_{k+1}-u_k)-K_{k-1/2}(u_k-u_{k-1})}{h^2},\quad K=K(z)>0,$$

*of the diffusion operator $L[u]=(Ku_z)_z$ with Dirichlet boundary conditions.*

[2] A matrix is called a Stieltjes matrix if it is a symmetric $M$-matrix.

**Proof.** By construction of $V$. □

As we see, $I-2U_V$ can be shown to be negative semidefinite for a rather wide class of tridiagonal matrices $V$. Assume now that $I-2U_V$ is negative semidefinite. To satisfy the stability condition (18) for the ROS1-AMF+ scheme we want $(\tau/2)R(I-2U_V)$ to be positive definite. This is true for the case $R=\lambda I$ (test problem (15)) and, as discussed in [5], is very likely to be true for the case $R=D$ (test problem (16)) since the diagonal elements of $D$ usually vary smoothly.

Thus we conclude that ROS-AMF+ can be expected to provide good stability in real-life situations. Unfortunately, we do not know how to extend these stability results to the second- and third-order Rosenbrock schemes ROS2 and ROS3. We note, however, that scalar case stability analysis of Verwer et al. [36] shows $A$-stability of ROS2-AMF (application of AMF leads to the loss of $L$-stability). Since we can expect that AMF+ is a better approximation to $\boldsymbol{I}-\tau\boldsymbol{J}$ than the standard AMF, we can also hope that stability properties of ROS2-AMF+ will be attractive too.

## 4. Other ways to solve the linear systems

In this section, we report on our experience with two other possible ways to approximately solve the linear systems (2).

### 4.1. AMFe: economical AMF

Standard AMF (3) gives an $\mathcal{O}(\tau^2)$ approximation to $\boldsymbol{I}-\tau\boldsymbol{J}$:

$$(\boldsymbol{I}-\tau\boldsymbol{R})(\boldsymbol{I}-\tau\boldsymbol{V})=\boldsymbol{I}-\tau\boldsymbol{J}+\tau^2\boldsymbol{R}\boldsymbol{V}. \tag{21}$$

A second-order approximation can also be achieved with the following more general class of AMF:

$$\boldsymbol{I}-\tau\boldsymbol{J}\approx(\boldsymbol{I}-\tau(\boldsymbol{R}_1+\boldsymbol{V}_1))(\boldsymbol{I}-\tau(\boldsymbol{R}_2+\boldsymbol{V}_2)),$$
$$\boldsymbol{R}=\boldsymbol{R}_1+\boldsymbol{R}_2,\quad \boldsymbol{V}=\boldsymbol{V}_1+\boldsymbol{V}_2. \tag{22}$$

When the number of vertical layers $n_z$ in the model is large, say more than 30, LU factorization of $n_z\times n_z$ diagonal blocks of $\boldsymbol{I}-\tau\boldsymbol{V}$ can become rather expensive. The LU factorization of $\boldsymbol{I}-\tau\boldsymbol{V}$ can be avoided if one chooses in (22)

$$\boldsymbol{R}_1=\boldsymbol{R},\quad \boldsymbol{R}_2=0,$$
$$\boldsymbol{V}_1=\boldsymbol{V}_{\mathrm{L}}\equiv\text{lower triangular part of }\boldsymbol{V},$$
$$\boldsymbol{V}_2=\boldsymbol{V}_{\mathrm{U}}\equiv\text{upper triangular part of }\boldsymbol{V}$$

which leads to the following economical AMF (AMFe):

$$\boldsymbol{I}-\tau\boldsymbol{J}\approx(\boldsymbol{I}-\tau(\boldsymbol{V}_{\mathrm{L}}+\boldsymbol{R}))(\boldsymbol{I}-\tau\boldsymbol{V}_{\mathrm{U}}). \tag{23}$$

The sparsity patterns of these matrix factors coincide with those of AMF+ (see Fig. 2).

Table 1
Computational costs of AMF and AMFe (costs associated with reactions depend on sparsity of $\boldsymbol{R}$ and are not specified)

| | Reaction costs | Vertical mixing costs | |
|---|---|---|---|
| AMF | $n_z$ LU factorizations | $n_t$ LU factorizations | |
| | of sparse $n_t \times n_t$ blocks, | of full $n_t \times n_t$ blocks: | $\frac{2}{3} n_t n_z^3$ flops |
| | backsolves | backsolves: | $n_t n_z(n_z+1)$ flops |
| AMFe | Same as for AMF | Backsolves: | $n_t n_z^2$ flops |

The main diagonals in $\boldsymbol{V}_{\mathrm{L}}$ and $\boldsymbol{V}_{\mathrm{U}}$ are computed in the following way. Each diagonal element in $\boldsymbol{V}_{\mathrm{L}}$ and $\boldsymbol{V}_{\mathrm{U}}$ is first set equal to the sum of the off-diagonal elements of its column taken with the opposite sign. To assure that

$$\mathrm{Diag}(\boldsymbol{V}) = \mathrm{Diag}(\boldsymbol{V}_{\mathrm{L}}) + \mathrm{Diag}(\boldsymbol{V}_{\mathrm{U}}),$$

the diagonals are then updated as

$$\begin{aligned} D^{+} &:= \mathrm{Diag}(\boldsymbol{V}) - \mathrm{Diag}(\boldsymbol{V}_{\mathrm{L}}) - \mathrm{Diag}(\boldsymbol{V}_{\mathrm{U}}),\\ \mathrm{Diag}(\boldsymbol{V}_{\mathrm{L}}) &:= \mathrm{Diag}(\boldsymbol{V}_{\mathrm{L}}) + \tfrac{1}{2} D^{+},\\ \mathrm{Diag}(\boldsymbol{V}_{\mathrm{U}}) &:= \mathrm{Diag}(\boldsymbol{V}_{\mathrm{U}}) + \tfrac{1}{2} D^{+}. \end{aligned} \tag{24}$$

Since $-\boldsymbol{V}$ is an $M$-matrix, with this choice of diagonals matrices $-\boldsymbol{V}_{\mathrm{L}}$ and $-\boldsymbol{V}_{\mathrm{U}}$ are (possibly singular) $M$-matrices too. As a consequence, matrices $(\boldsymbol{I}-\tau\boldsymbol{V}_{\mathrm{L}})^{-1}$ and $(\boldsymbol{I}-\tau\boldsymbol{V}_{\mathrm{U}})^{-1}$ are elementwise nonnegative, just as the matrix $(\boldsymbol{I}-\tau\boldsymbol{V})^{-1}$ is. This property is desirable for preserving positivity.

A simple stability analysis for the ROS1-AMFe scheme, similar to the analysis for ROS-AMF+ from the previous section, can be found in [5]. This analysis shows that the scheme has good stability properties in practical situations. The costs of AMFe are summarized in Table 1.

Because of the explicit nature of AMFe, we expect that the accuracy properties of AMFe-based schemes will be poor. The poor accuracy properties are often encountered in explicit unconditionally stable schemes, as e.g. in the Du Fort–Frankel scheme [22] and in a scheme of Samarskii similar to ROS1-AMFe where the spatially discretized operator is split into lower and upper triangular matrices [25]. However, since the step sizes typically used in air pollution models are not very large with respect to the vertical mixing process (cf. (6)), one may hope that the accuracy will not degrade too much. Moreover, one may consider the following way to repair the accuracy of AMFe: if it is known that an active vertical mixing takes place in the layers $k_1,\ldots,k_2$ ($k_1 < k_2$) then we may leave elements of the submatrix of $V$ occupying the $k_1,\ldots,k_2$ rows and columns unsplit in the $\boldsymbol{V}_{\mathrm{U}}$ part. This would lead to the sparsity structure shown in Fig. 3.

### 4.2. Experience with GMRES: no gain

Here we report briefly on our experience with solving the linear systems (2) by a modern Krylov iterative scheme. As an option, we have used the AMF matrix $(\boldsymbol{I}-\tau\boldsymbol{R})(\boldsymbol{I}-\tau\boldsymbol{V})$ as a preconditioner. We have made numerical experiments to compare ROS2-AMF against ROS2 equipped with the

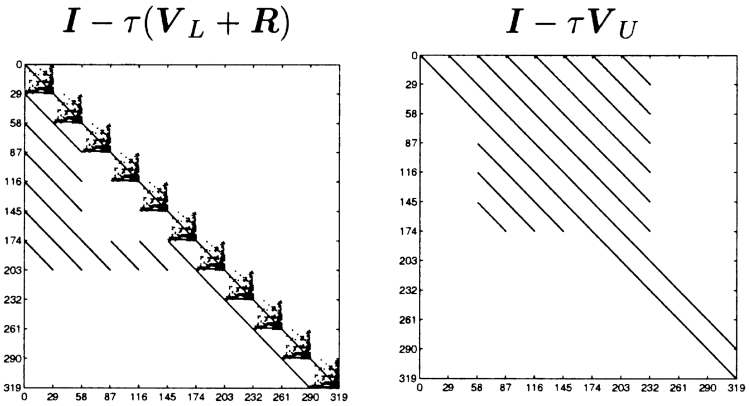


Fig. 3. Sparsity structure of the matrix factors in the "repaired" AMFe. $k_1 = 4$ and $k_2 = 6$.

AMF-preconditioned nonrestarted GMRES method as a linear solver [23]. When the Jacobian matrix is not symmetric, among all modern Krylov iterative solvers, GMRES is an ideal candidate for use in time integration. First of all, nonrestarted GMRES is guaranteed to converge [23] thus turning ROS-GMRES into the exact Jacobian ROS2 integrator with all its nice stability properties. Secondly, since the number of iterations will normally be kept restricted ($\leqslant 20$ in most cases), the restarting often applied in GMRES for a large number of iterations can be avoided. Hence, the only serious drawback of full GMRES, growth of work and memory requirements with the number of iterations, will not be pronounced. Note that nonrestarted GMRES is an optimal scheme (it minimizes the residual norm among all other Krylov subspace methods) which is superior (in number of iterations) to other popular schemes for nonsymmetric matrices as BiCGSTAB [34], BiCGStab($\ell$) [29], QMR [9], and TFQMR [8]. These schemes were designed as a cheaper alternative to the full GMRES and do not have the optimality property.

The results of our tests were unfavorable for ROS2-GMRES. Due to the efficient use of sparsity in $\boldsymbol{I} - \tau\boldsymbol{R}$, for typical values of $n_z$ and $n_t$, the AMF solution (4) is done very cheaply, with the costs comparable to one matrix-vector multiplication $\boldsymbol{y} := (\boldsymbol{I} - \tau\boldsymbol{J})\boldsymbol{x}$. This means that doing just one unpreconditioned iteration of GMRES or any other Krylov method per time step is twice as expensive as AMF action (4). Furthermore, one AMF-preconditioned GMRES iteration implies a factor four increase in costs. One could hope that taking a larger step size for the GMRES-based scheme might make it more competitive. However, the step size typically used for ROS2-AMF ($\Delta t \approx 30$ min) is already nearly the maximum one for capturing important solution properties. At least for this particular problem, this leaves no chance to any Krylov iterative solver. Even if we assume that an ideal Krylov solver exists that converges in one iteration and costs for the preconditioning are negligible, the total costs per time step will be at least twice as high as for ROS2-AMF.

The unpreconditioned GMRES performed very poor: the residual norm was hardly damped within a reasonable number of iterations. The AMF-preconditioned GMRES performed well, converging within about 10 iterations, allowing the scheme to work with a step size larger than for ROS2-AMF (up to 40–45 min) but also providing a slightly more accurate solution than ROS2-AMF. However, this was by far not enough to compensate for the extra costs in GMRES.

## 5. Numerical experiments

Along with the variants of AMF considered above, one could also use the following alternative factorizations (cf. (3), (23) and (9)):

$$\begin{aligned}
&\text{AMF}: \boldsymbol{I}-\tau\boldsymbol{J}\approx(\boldsymbol{I}-\tau\boldsymbol{V})(\boldsymbol{I}-\tau\boldsymbol{R}),\\
&\text{AMFe}: \boldsymbol{I}-\tau\boldsymbol{J}\approx(\boldsymbol{I}-\tau\boldsymbol{V}_{\mathrm{L}})(\boldsymbol{I}-\tau(\boldsymbol{V}_{\mathrm{U}}+\boldsymbol{R})),\\
&\text{AMF}+: \boldsymbol{I}-\tau\boldsymbol{J}\approx\tilde{\boldsymbol{L}}_V(\tilde{\boldsymbol{U}}_V-\tau\boldsymbol{R}),\quad \tilde{\boldsymbol{L}}_V\tilde{\boldsymbol{U}}_V=\boldsymbol{I}-\tau\boldsymbol{V},\\
&\mathrm{Diag}(\tilde{\boldsymbol{L}}_V)=\boldsymbol{I}.
\end{aligned}\tag{25}$$

We will refer to these AMF versions as the R2 versions (indicating that $\boldsymbol{R}$ appears now in the second factor). Correspondingly, the standard AMF (3), AMF+ (9), and AMFe (23) will be called the R1 versions. In our numerical experiments we have tested matrix factorizations in both the R1 and R2 modes.

As a test problem we take system (1) with the chemistry model carbon bond mechanism IV (CBM-IV) involving $n_t = 32$ tracers. All parameters are chosen in the same way as in the CBM-IV urban scenario from [27], i.e. emissions are high. Our vertical mixing matrix $\boldsymbol{V}$ is taken from the TM3 code [31], $-\boldsymbol{V}$ is a columnwise weakly diagonally dominant $M$-matrix. Unlike [36], where the vertical mixing matrix was tridiagonal, coming from a three-point discretization of the diffusion operator, our matrix $\boldsymbol{V}$ is dense. The way matrix $\boldsymbol{V}$ is computed is described in detail in [2]. Note, however, that the scavenging effect has not been included in our model and that all tracers are vertically mixed.

The time interval is 5 days. The initial conditions $\boldsymbol{y}(0)=\boldsymbol{y}_0$ are chosen in the same way as in [36]: $\boldsymbol{y}_0$ is the solution after a 1-day very accurate time integration with a reasonable initial value vector. During the integration, matrix $\boldsymbol{V}$ is read from disk every 6 h and its LU decomposition is recomputed (except for AMFe, where the LU decomposition is not carried out).

We compare solutions of ROS2 applied with each of the three AMF variants (AMF, AMF+, AMFe) against the solution of the full ROS2 where no AMF is used ($\boldsymbol{A}=\boldsymbol{J}$ in (5)). This is done for a large fixed $\Delta t = 1800$ s (=30 min). The error measured with respect to the full ROS2 is triggered only by the inexact AMF solves, the contribution of the local error of ROS2 is not of interest in our study. Since the full ROS2 scheme has proven a reliable and robust method for atmospheric chemistry [2,4,35,36], we choose to use the solution of the full ROS2 as a reference.

In our computations we use clipping: negative concentrations that occasionally occur are set to zero. Normally, negative values occur rarely and are relatively small, so that the mass conservation is almost preserved. Clipping is often used for atmospheric models.

### 5.1. Testing AMF+ versus AMF

For most of the tracers, both ROS2-AMF and ROS2-AMF+ produce solutions hardly different from the solution of the full ROS2 (see Fig. 4). For eleven tracers, most of which are fast reacting, both ROS2-AMF and ROS2-AMF+ produce significant errors. Comparison of ROS2 solution with a solution obtained with a very small time step size suggests that these errors are a consequence of using AMF. Similar, even more favorable for ROS2-AMF observations were made in [2] for

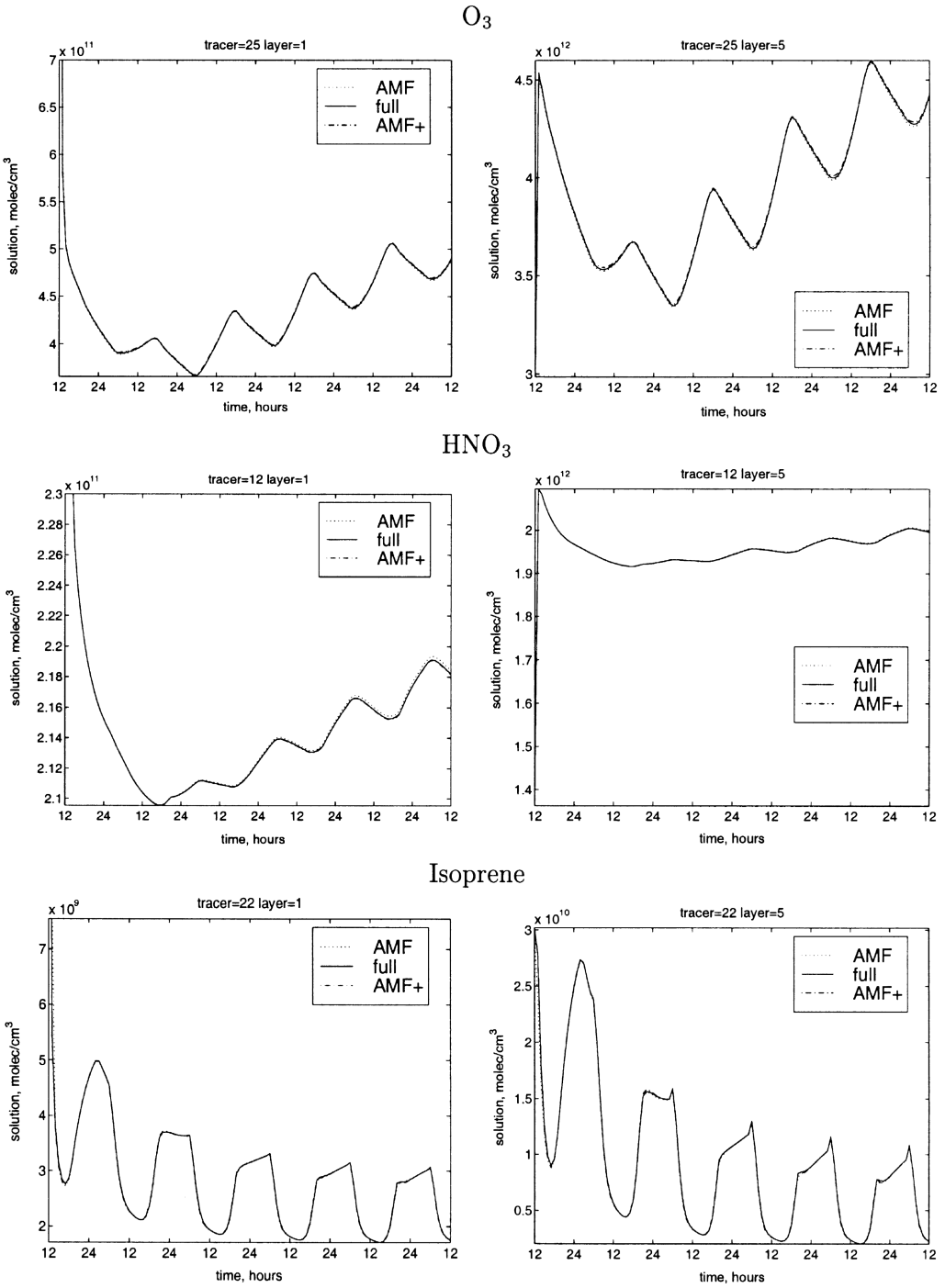


Fig. 4. Solutions of ROS2 (solid line), ROS2-AMF (dotted line) and ROS2-AMF+ (dash-dotted line) for tracers $O_3$, $HNO_3$ and isoprene, layers 1 (left) and 5 (right). Version R1 of AMF and AMF+ is used.

the TM3 model: there, the difference between ROS2 and ROS2-AMF solutions was negligible for almost all tracers. The more accurate behavior of ROS2-AMF in [2] can be explained by the fact that in TM3 several fast reacting tracers do not participate in the vertical mixing, thus reducing the AMF error.

Comparing AMF and AMF+, we clearly see that ROS2-AMF+ is typically significantly more accurate than ROS2-AMF (see Fig. 5). In fact, we see that ROS2-AMF+ performs worse than ROS2-AMF only for one tracer and then only for several, nonsurface layers. In overall, ROS2-AMF+ is pronouncedly more accurate, especially for the eleven tracers for which larger errors are observed. This is true for both R1 and R2 versions of AMF and AMF+. It is not possible to say which version, R1 or R2, is preferable. In general, the R1 version seems to be more accurate. However, the R2 version seems to be more stable: without clipping ROS2-AMF remains stable only in the R2 mode. (ROS2-AMF+ can work without clipping in both R1 and R2 modes.) To complete the whole integration, both ROS2-AMF and ROS2-AMF+ required roughly the same CPU time, about 3.5 s on a PC with an AMD-K6 processor.

### 5.2. Testing AMFe

Unlike ROS2-AMF and ROS2-AMF+, with the step size $\Delta t = 1800$ s ROS2-AMFe is unacceptably inaccurate (the relative error is $\sim 100\%$). Reduction of the step size by a factor two does not sufficiently help. However, with the step size $\Delta t = 450$ s ROS2-AMFe works reasonably well (Fig. 6). The error is then only significant for the same eleven fast tracers, just as for ROS2-AMF and ROS2-AMF+. Again, switching between the R1 and R2 versions does not influence the situation much. Note that for $\Delta t = 450$ s we have $\Delta t \|\boldsymbol{V}\|_2 \approx 6.13$, so that the vertical mixing still could not be treated explicitly (in the ROS2 framework, this can be straightforwardly implemented, see e.g. [36]).

The question is whether ROS2-AMFe, applied with a step reduced by a factor four, would still be cheaper than ROS2-AMF or ROS2-AMF+ in terms of the CPU time. In our tests the all-round CPU time of ROS2-AMFe was approximately 7 s, twice as much as the CPU time of ROS2-AMF and ROS2-AMF+. This, however, can be quite different. Indeed, let $\Delta t$ be the step size of ROS2-AMF, $T$ be the total integration time and the vertical mixing be updated once in a $\Delta t_{\mathrm{vmix}}$ time (in our tests $\Delta t_{\mathrm{vmix}} = 6$ h). Assume now that ROS2-AMFe works well with the step size $\Delta t/s$, $s \geqslant 1$ and $\tilde{t}_{\mathrm{LU}}$ and $\tilde{t}_{\mathrm{step}}$ are the CPU times to compute LU factorization of $\boldsymbol{V}$ and make a ROS2 step, respectively. A rough estimation shows that ROS2-AMFe will be faster if

$$\frac{sT}{\Delta t}\,\tilde{t}_{\mathrm{step}} < \frac{T}{\Delta t}\,\tilde{t}_{\mathrm{step}} + \frac{T}{\Delta t_{\mathrm{vmix}}}\,\tilde{t}_{\mathrm{LU}}$$

or

$$(s-1)\tilde{t}_{\mathrm{step}} < \frac{\Delta t}{\Delta t_{\mathrm{vmix}}}\,\tilde{t}_{\mathrm{LU}}.$$

This can easily be true in the future generation air pollution models, where the number of vertical layers is to be $\sim \mathcal{O}(100)$ (recall that $\tilde{t}_{\mathrm{LU}} \sim \mathcal{O}(n_z^3)$) and the vertical mixing matrix is to be updated more often ($\Delta t_{\mathrm{vmix}}$ is small).

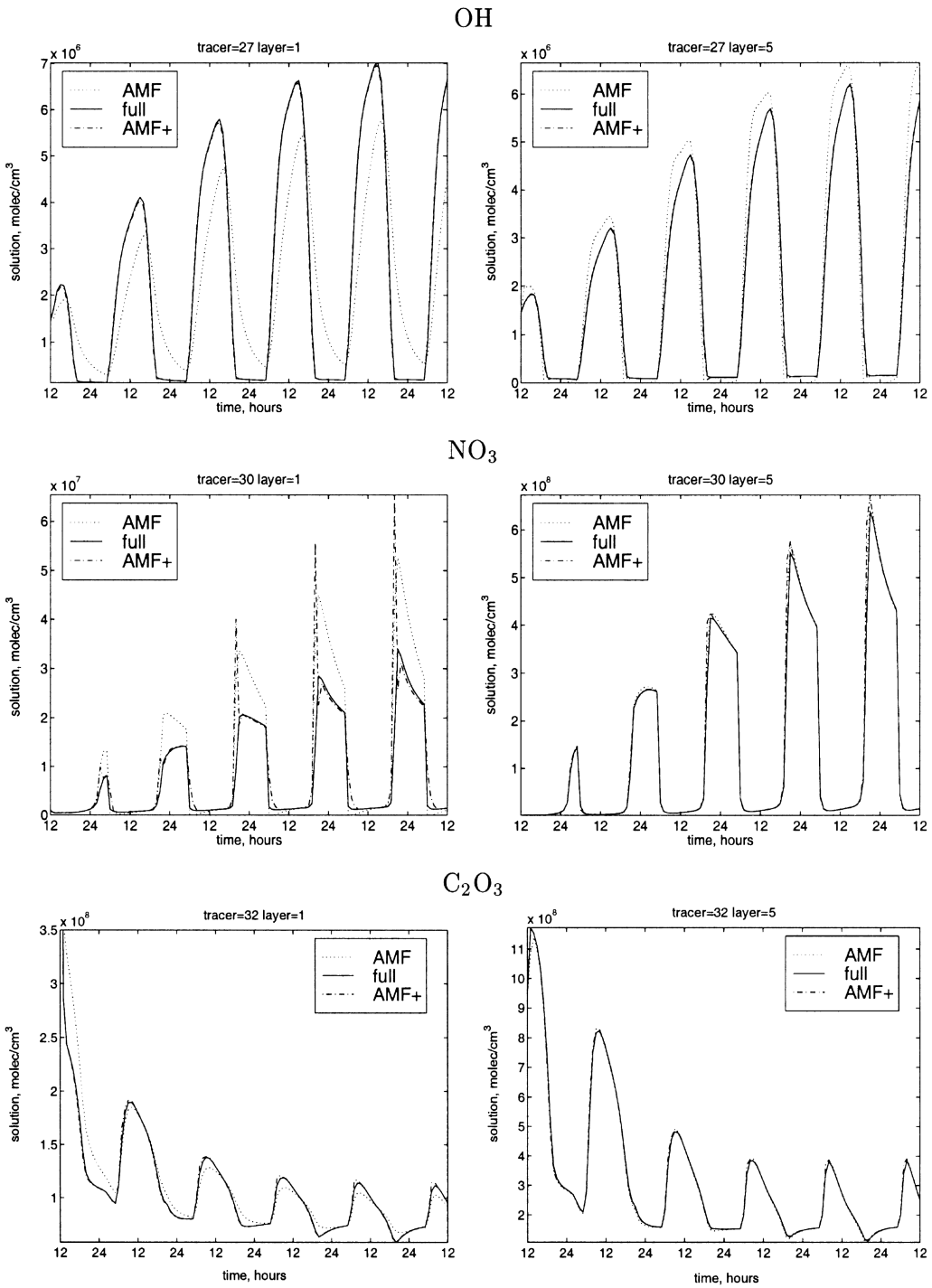


Fig. 5. Solutions of ROS2 (solid line), ROS2-AMF (dotted line) and ROS2-AMF+ (dash-dotted line) for tracers OH, $NO_3$ and $C_2O_3$, layers 1 (left) and 5 (right). Version R1 of AMF and AMF+ is used.

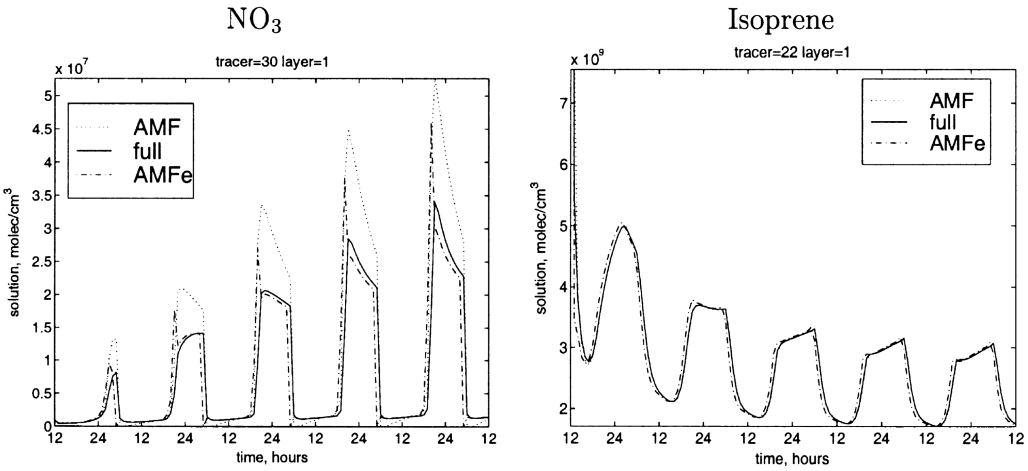


Fig. 6. Solutions of ROS2 (solid line), ROS2-AMF (dotted line) and ROS2-AMFe (dash-dotted line) for tracers $NO_3$ and isoprene, layer 1. Version R1 of AMF and AMFe is used.

As shown in [5], performance of the AMFe could be also improved by applying the modification shown in Fig. 3. We have good experience with using this "repaired" AMFe but this is rather ad hoc and case-dependent.

### 5.3. Parallel computation aspects

Since system (1) has to be treated implicitly, its solution is difficult to parallelize. This also applies to ROS2 combined with AMF, AMFe, or AMF+. In air pollution modeling one often distributes the 3D physical domain horizontally among the processors, so that each processor has the whole range of grid cells in $z$-direction (see e.g., [31,35,37]). Systems (1) are then solved locally within one processor. The use of ROS2-AMF with constant step sizes, as advocated in this paper, allows to avoid the load balancing problems.

## 6. Conclusions

The new AMF called AMF+ has been proposed and shown, both analytically and numerically, to give a significant profit in accuracy as compared against standard AMF. AMF+ does not require any additional computational work. The fact that we deal with matrices which in practical situations do not commute hinder the stability analysis. The analysis is done only for simplified test problems; it shows that AMF+ provides good stability in practical situations.

In another, cheaper AMF called AMFe (economical) the block LU factorization of $\boldsymbol{I} - \tau \boldsymbol{V}$ is avoided. This approach gives a scheme which is explicit with respect to the vertical mixing, stable but rather inaccurate. In our tests AMFe performed satisfactory only for a smaller step size, thus loosing in CPU time to AMF+ and AMF. However, for a larger number of vertical layers $n_z$ AMFe

can become attractive since the avoided costs are $\mathcal{O}(n_z^3)$. Moreover, inaccuracy of AMFe can be cured by applying the modification as shown in Fig. 3.

We have also reported on our experience with schemes based on preconditioned GMRES. These schemes turn out to be robust but more expensive for air pollution modeling than AMF-based schemes.

## Acknowledgements

This work is a part of a larger joint effort, sponsored by the Netherlands Organization for Scientific Research (NWO) under Grant No. 613-302-040, to enhance the TM3/TM5 global model [31,32]. We gratefully acknowledge the TM3/TM5 development team, in particular, Maarten Krol and Wouter Peters from IMAU (Utrecht).

We thank our colleagues Patrick Berkvens, Jos van Dorsselaer and Willem Hundsdorfer for valuable comments that helped us in the preparation of the paper.

## References

[1] R.M. Beam, R.F. Warming, An implicit finite-difference algorithm for hyperbolic systems in conservation-law form, J. Comput. Phys. 22 (1976) 87–110.
[2] P.J.F. Berkvens, M.A. Botchev, M.C. Krol, W. Peters, J.G. Verwer, Solving vertical transport and chemistry in air pollution models, in: D. Chock, G. Carmichael (Eds.), Atmospheric Modeling, Vol. 130 of IMA Volumes in Mathematics and its Applications, Springer, Berlin, 2002, pp. 1–20.
[3] P.J.F. Berkvens, M.A. Botchev, J.G. Verwer, On the efficient treatment of vertical mixing and chemistry in air pollution modelling, in: R. Owens (Ed.), CD-ROM Proceedings of the 16th IMACS World Congress, Lausanne, 2000.
[4] J.G. Blom, J.G. Verwer, A comparison of integration methods for atmospheric transport-chemistry problems, J. Comput. Appl. Math. 126 (2000) 381–396.
[5] M.A. Botchev, J.G. Verwer, Improving approximate matrix factorizations for implicit time integration in air pollution modelling, CWI Report MAS-R0031, Amsterdam, 2000.
[6] K. Dekker, J.G. Verwer, Stability of Runge–Kutta Methods for Stiff Non-linear Differential Equations, North-Holland, Elsevier, Amsterdam, 1984.
[7] E.G. D'yakonov, Difference systems of second-order accuracy with a divided operator for parabolic equations without mixed derivatives, USSR Comput. Math. Phys. 4 (5) (1964) 206–216.
[8] R.W. Freund, A transpose-free quasi-minimal residual algorithm for non-Hermitian linear systems, SIAM J. Sci. Statist. Comput. 14 (1993) 470–482.
[9] R.W. Freund, N.M. Nachtigal, QMR: a quasi-minimal residual method for non-Hermitian linear systems, Numer. Math. 60 (1991) 315–339.
[10] A. Gerisch, J.G. Verwer, Operator splitting and approximate factorization for taxis-diffusion-reaction models, Appl. Numer. Math. 42 (2002) 159–176.
[11] S.K. Godunov, V.S. Ryabenkii, Difference Schemes. An Introduction to the Underlying Theory, Elsevier, Amsterdam, 1987.
[12] E. Hairer, G. Wanner, Solving Ordinary Differential Equations II. Stiff and Differential-Algebraic Problems, Springer Series in Computational Mathematics, Vol. 14, 2 Edition, Springer, Berlin, 1996.
[13] M. Heimann, The global atmospheric tracer model TM2, Technical Report 10, Deutches Klimarechenzentrum (DKRZ), Hamburg, 1995.
[14] W. Hundsdorfer, Accuracy and stability of splitting with stabilizing corrections, CWI Report MAS-R9935, Amsterdam, 1999.

[15] C. Kessler. Entwicklung eines effizienten Lösungverfahrens zur modellmässigen Beschreibung der Ausbreitung und chemischen Umwandlung reaktiver Luftschadstoffe, Ph.D. Thesis, Facultät für Maschinenbau der Universtät Karlsruhe, Aachen, 1995.
[16] O. Knoth, R. Wolke, A comparison of fast chemical kinetic solvers in a simple vertical diffusion model, in: S.-V. Gryning, M. Millán (Eds.), Air Pollution Modelling and its Application, Vol. X, Plenum Press, New York, 1994, pp. 287–294.
[17] O. Knoth, R. Wolke, Implicit–explicit Runge–Kutta methods for computing atmospheric reactive flows, Appl. Numer. Math. 28 (1998) 327–341.
[18] D. Lanser, J.G. Blom, J.G. Verwer, Time integration of the shallow water equations in spherical geometry, J. Comput. Phys. 171 (2001) 373–393.
[19] B. Lastdrager, B. Koren, J.G. Verwer, Solution of time-dependent advection-diffusion problems with the sparse-grid combination technique and a Rosenbrock solver, Comput. Methods Appl. Math. 1 (1) (2001) 86–98.
[20] http://www.cwi.nl/~gollum/lotos/, LOTOS: LOng-term ozone simulation, CWI, Amsterdam.
[21] D.W. Peaceman, H.H. Rachford Jr., The numerical solution of parabolic and elliptic differential equations, J. Soc. Indust. Appl. Math. 3 (1955) 28–41.
[22] R.D. Richtmyer, K.W. Morton, Difference Methods for Initial-Value Problems, 2nd Edition, Interscience Publishers, Wiley, New York–London–Sydney, 1967 (Interscience Tracts in Pure and Applied Mathematics, No. (4)).
[23] Y. Saad, M.H. Schultz, GMRES: a generalized minimal residual algorithm for solving nonsymmetric linear systems, SIAM J. Sci. Statist. Comput. 7 (3) (1986) 856–869.
[24] A.A. Samarskii, Regularization of difference schemes, USSR Comput. Math. Math. Phys. 7 (1967) 62–93.
[25] A.A. Samarskii, Theorie der Differenzenverfahren, Akademische Verlagsgesellschaft Geest & Portig K.-G., Leipzig, 1984 (trans. from the Russian by Gisbert Stoyan).
[26] A. Sandu, F.A. Potra, G.R. Carmichael, V. Damian, Efficient implementation of fully implicit methods for atmospheric chemical kinetics, J. Comput. Phys. 129 (1996) 101–110.
[27] A. Sandu, J.G. Verwer, J.G. Blom, E.J. Spee, G.R. Carmichael, Benchmarking stiff ODE solvers for atmospheric chemistry problems II: Rosenbrock solvers, Atmos. Environ. 31 (1997) 3459–3472.
[28] A. Sandu, J.G. Verwer, M. van Loon, G.R. Carmichael, F.A. Potra, D. Dabdub, J.H. Seinfeld, Benchmarking stiff ODE solvers for atmospheric chemistry problems I: implicit versus explicit, Atmos. Environ. 31 (1997) 3151–3166.
[29] G.L.G. Sleijpen, D.R. Fokkema, BiCGStab($\ell$) for linear equations involving unsymmetric matrices with complex spectrum, Electron. Trans. Numer. Anal. 1 (1993) 11–32.
[30] B. Sportisse, An analysis of operator splitting techniques in the stiff case, J. Comput. Phys. 161 (1) (2000) 140–168.
[31] http://www.phys.uu.nl/~peters/TM3/TM3S.html, the TM3 model homepage. IMAU, Utrecht University, Utrecht.
[32] http://www.phys.uu.nl/~peters/TM5/, the TM5 model: The next generation in atmospheric modeling. IMAU, Utrecht University, Utrecht.
[33] P.J. vander Houwen, B.P. Sommeijer, Approximate factorization for time-dependent partial differential equations, J. Comput. Appl. Math. 128 (1–2) (2001) 447–466 (Numerical analysis 2000, Vol. VII, Partial differential equations).
[34] H.A. vander Vorst, BiCGSTAB: a fast and smoothly converging variant of BiCG for the solution of nonsymmetric linear systems, SIAM J. Sci. Statist. Comput. 13 (2) (1992) 631–644.
[35] J.G. Verwer, W. Hundsdorfer, J.G. Blom, Numerical time integration for air pollution models, Surveys Math. Ind. 10 (2002) 107–174.
[36] J.G. Verwer, E.J. Spee, J.G. Blom, W. Hundsdorfer, A second-order Rosenbrock method applied to photochemical dispersion problems, SIAM J. Sci. Comput. 20 (1999) 456–480.
[37] Z. Zlatev, Computer Treatment of Large Air Pollution Models, Kluwer Academic Publishers, Dordrecht, 1995.